Check for updates

Granule exocytosis is required for platelet spreading: differential sorting of α-granules expressing VAMP-7

Christian G. Peters,[1] Alan D. Michelson,[2] and Robert Flaumenhaft[1]

[1]Division of Hemostasis and Thrombosis, Department of Medicine, Beth Israel Deaconess Medical Center, Harvard Medical School, Boston, MA; and [2]Center for Platelet Research Studies, Division of Hematology/Oncology, Children's Hospital Boston, Dana-Farber Cancer Institute, Harvard Medical School, Boston, MA

There has been recent controversy as to whether platelet α-granules represent a single granule population or are composed of different subpopulations that serve discrete functions. To address this question, we evaluated the localization of vesicle-associated membrane proteins (VAMPs) in spread platelets to determine whether platelets actively sort a specific subpopulation of α-granules to the periphery during spreading. Immunofluorescence microscopy demonstrated that granules expressing VAMP-3 and VAMP-8 localized to the central granulomere of spread platelets along with the granule cargos von Willebrand factor and serotonin. In contrast, α-granules expressing VAMP-7 translocated to the periphery of spread platelets along with the granule cargos TIMP2 and VEFG. Time-lapse microscopy demonstrated that α-granules expressing VAMP-7 actively moved from the granulomere to the periphery during spreading. Platelets from a patient with gray platelet syndrome lacked α-granules and demonstrated only minimal spreading. Similarly, spreading was impaired in platelets obtained from *Unc13d*^{Jinx} mice, which are deficient in Munc13-4 and have an exocytosis defect. These studies identify a new α-granule subtype expressing VAMP-7 that moves to the periphery during spreading, supporting the premise that α-granules are heterogeneous and demonstrating that granule exocytosis is required for platelet spreading. (*Blood*. 2012;120(1):199-206)

Introduction

Platelets are replete with granules containing cargo that is required for platelet function in hemostasis, thrombosis, inflammation, angiogenesis, and malignancy.[1-4] Platelet granule types include α-granules, dense granules, and lysosomes. Of these granule types, the α-granule is by far the most abundant with 50 to 80 granules/platelet, compared with 3 to 6 dense granules/platelet and 0 to 3 lysosomes/platelet. Recent studies indicate that α-granules may not constitute a homogenous population. There is evidence that α-granule subpopulations can be distinguished on the basis of morphology,[5] cargo type,[6-8] and response to agonists.[7-10] However, experiments using high resolution immunofluorescence microscopy have raised the possibility that the distribution of cargo among α-granules is largely stochastic and that the apparent segregation observed by standard immunofluorescence microscopy could result from segregation within granules.[11,12]

Although the study of α-granule heterogeneity has focused primarily on the localization and release of granule cargo, granules also serve an essential role in membrane remodeling. In nucleated cells, granules provide an internal reservoir of membrane to expand and reshape the plasma membrane during cell movement,[13] membrane resealing,[14,15] neurite outgrowth,[16-18] and development of the phagocytotic cup in macrophages.[19,20] Different subpopulations of granules demonstrate different behaviors during membrane remodeling. Recent studies demonstrate that these different granule types can be distinguished by the vesicle-associated membrane proteins (VAMPs) that they express.[21-24] VAMPs reside on the cytosolic face of granules and localize to granule subpopulations that differ in their location and function.[25-30] Although we and others have demonstrated a role for VAMPs in platelet exocytosis,[2,31-33] their relative distribution and function in platelet spreading has not been previously explored.

Transmission electron microscopy has demonstrated that when a platelet contacts a substrate, its granules coalesce in a central granulomere that is surrounded by a microtubule ring.[34] However, alternative methods of imaging, such as differential interference contrast (DIC) microscopy, atomic force microscopy, and scanning electron microscopy demonstrate organelles in the periphery of the spread platelet.[35,36] We postulated that a subpopulation of α-granules were among the peripheral organelles in spread platelets and that platelets actively sort this subpopulation of α-granules to the periphery during spreading.

To determine whether a distinct subpopulation of platelet α-granules sorts to the platelet periphery during platelet spreading, we monitored granule dynamics and evaluated the localization of VAMPs during platelet spreading. Our results demonstrate that a subpopulation of α-granules expressing VAMP-7 segregate from granules expressing VAMP-3 or VAMP-8 in spread platelets. Although granules expressing VAMP-3 and VAMP-8 localize to the central granulomere of the spreading platelet, granules expressing VAMP-7 translocate to the periphery. We also show that platelets either lacking α-granules or defective in their ability to secrete granules fail to spread normally. These results demonstrate that α-granule exocytosis is required for platelet spreading and identify a new α-granule subtype that expresses VAMP-7 and moves to the periphery during spreading. Our observations support the premise that α-granules are heterogeneous and demonstrate that

Submitted October 31, 2011; accepted May 1, 2012. Prepublished online as *Blood* First Edition paper, May 15, 2012; DOI 10.1182/blood-2011-10-389247.

The online version of this article contains a data supplement.

The publication costs of this article were defrayed in part by page charge payment. Therefore, and solely to indicate this fact, this article is hereby marked "advertisement" in accordance with 18 USC section 1734.

© 2012 by The American Society of Hematology

Downloaded from http://ashpublications.net/blood/article-pdf/120/1/199/1356030/zh802712000199.pdf by guest on 20 May 2024

different VAMP isoforms associate with functionally discrete α-granule subpopulations.

Methods

Platelet preparation

Blood was obtained from healthy donors who had not ingested aspirin or NSAIDs in the 2 weeks before donation using a protocol approved by the institutional review board of Beth Israel Deaconess Medical Center (BIDMC). Platelets were isolated by centrifugation followed by gel filtration of platelet-rich plasma as previously described.[37]

Patients

The patient with gray platelet syndrome (GPS) is a 5-year-old female from Abu Dhabi with a history of mild thrombocytopenia. Her blood smear demonstrated no α-granules. The diagnosis of GPS was confirmed by electron microscopy. Immunofluorescence microscopy demonstrated expression of VAMP-3, VAMP-7, and VAMP-8 (supplemental Figure 1, available on the *Blood* Web site; see the Supplemental Materials link at the top of the online article). The patient with Hermansky-Pudlak syndrome (HPS) is a 46-year-old female of Puerto Rican heritage with subtype 1 HPS. Use of platelets from control subjects and patients with HPS and GPS was approved by the institutional review boards of BIDMC and Children's Hospital, Boston.

Mice

The *Unc13d*^{Jinx} mice (MMRRC: 016137) on a C57Bl/6J background were purchased from Mutant Mouse Regional Resource Center at the University of California, Davis. Age- and sex-matched wild-type C57Bl/6J mice were purchased from The Jackson Laboratory. All animal use was approved by the BIDMC Institutional Animal Care and Use Committee.

Antibodies

All antibodies were purchased from commercial resources and used at a concentration that was saturating. Isotype-matched controls were used to confirm antibody specificity and evaluate nonspecific binding. In addition, as background controls, platelets were incubated with secondary antibody alone. Polyclonal antibodies to cellubrevin (VAMP-3), SYBL1 (VAMP-7), and monoclonal antibodies to von Willebrand factor (VWF) and vascular endothelial growth factor (VEGF) were purchased from Abcam. Mouse monoclonal antibodies directed at endobrevin (VAMP-8) were purchased from Novus Biologicals, and mouse monoclonal antibodies directed at platelet factor 4 (PF4) and tissue inhibitor of metalloproteinase 2 (TIMP2) were from R&D Systems. Rabbit polyclonal antibody to serotonin and mouse monoclonal antibody to thrombospondin were purchased from Thermo Fisher. Rabbit polyclonal antibody to platelet-derived growth factor (PDGF)–β was purchased from Santa Cruz. All samples were exposed to a secondary goat anti-rabbit or mouse antibody conjugated to Alexa Fluor 488 or 568 (Life Technologies).

Platelet spreading assay

Washed platelets were pelleted by centrifugation at 1200*g* for 10 minutes. The platelet pellet was resuspended in 5 mL of HEPES (*N*-2-hydroxyethylpiperazine-*N*′-2-ethanesulfonic acid)–Tyrode buffer (10mM HEPES, 140mM NaCl, 3mM KCl, 0.5mM $MgCl_2$, 5mM $NaHCO_3$, 10mM glucose, pH 7.4) and allowed to rest for a minimum of 20 minutes at 37°C. The platelet count was adjusted before seeding at 4×10^6/400 μL. Platelet suspension (400 μL) was applied to 12-mm glass coverslips that were precoated with poly-L-lysine (1 mg/mL), collagen (10 μg/cm^2), and fibronectin (5 μg/cm^2; Sigma-Aldrich) in 24-well cell culture plates. Platelets were allowed to adhere and spread for designated time periods (ranging from 0 to 30 minutes) at room temperature without shaking. The unbound platelets were removed by aspiration, followed by fixation using 4% paraformaldehyde in phosphate-buffered saline (PBS). Platelets were fixed for 15 minutes, washed with PBS and stored in immunofluorescence (IF) buffer (0.5 g bovine serum albumin, 0.25 mL 10% sodium azide, 5 mL goat serum, in 1× PBS) at 4°C until staining.

For visualization of actin structures, the high-affinity F-actin probe Alexa Fluor 568 phalloidin (Life Technologies) was used. Staining was performed using 7.5 μL of methanol stock solution prepared according to the manufacturer's suggested stock solution in 300 μL IF buffer. Coverslips were stained for 20 minutes at room temperature, washed twice, mounted onto glass slides with Aqua-Poly/Mount (Polysciences), and evaluated by fluorescence microscopy.

Live-cell microscopy

Platelet-rich plasma was collected as described previously. Secretory granules were labeled by incubating the platelets with Qtracker 565 nontargeted nanocrystals (Life Technologies) overnight, rotating at room temperature. Platelets were then washed by centrifugation (1200*g* for 10 minutes, resuspended in HEPES-Tyrode buffer) twice for removal of unincorporated nanocrystals and allowed to rest between washes for 20 minutes. For visualization of granule movement, real-time fluorescent microscopy was performed using an Olympus BX62 microscope (Olympus America) equipped with a 60× (NA = 1.42) Plan-Apo oil immersion objective and captured with an Orca-ER cooled CCD camera (Hamamatsu) at room temperature. Image acquisitions were controlled by iVision-Mac (Biovision Technologies) with a sampling time of 15 seconds. All images were exported as TIFF files and processed using ImageJ 1.44p Java 1.6.0_20 (32-bit) software.

Confocal microscopy

For colocalization experiments, 4.0×10^6 washed platelets were spun onto poly-L-lysine coated coverslips in 4% paraformaldehyde dissolved in PBS. Coverslips were washed twice with PBS and the platelets were permeabilized using 0.5% Triton-X-100. Samples were briefly washed and blocked overnight in IF buffer. After washing with PBS, platelets were incubated with the corresponding antibodies (1:100 dilutions) for 1 hour at room temperature. Primary antibodies were removed and Alexa Fluor conjugated anti–mouse/anti–rabbit antibodies (1:250 dilutions) were applied for 1 hour at room temperature. Confocal scanning laser microscopy was performed with a Zeiss LSM 510 Meta system confocal microscope (Carl Zeiss). Fluorescence images of 2 colors were captured sequentially using laser lines at 488 nm and 561 nm to prevent spectral overlap. Series of x-y images were collected along the z-axis at 0.25-μm intervals using a Plan-Apo 63× (NA = 1.4) oil immersion objective and an optical zoom of 2. Confocal micrographs were captured using Zeiss LSM 5 Version 4.0 software with service pack 1 and exported as TIFF files for further analysis.

Colocalization. Images for colocalization analysis were quantified using ImageJ 1.44p Java 1.6.0_20 (32-bit) software. JACoP (http://imagejdocu.tudor.lu/doku.php?id=plugin:analysis:jacop_2.0:just_another_colocalization_plugin:start) was used to process image stacks and allow an automated colocalization analysis. Statistical analysis of the correlation of the intensity values of 2-channels were plotted as scatter plots and the relationship between intensities of the 2 images was reported as the Pearson coefficient. To discriminate differences between partial colocalization, Manders coefficient analysis was completed using the JACoP plugin and reported as the proportion of signal one overlapping signal 2. The threshold was estimated as the value of background.

Surface area and perimeter analysis. For analysis of platelet spreading, ImageJ 1.44p Java 1.6.0_20 (32-bit) software was used to determine the surface areas and perimeters of platelets. Exported TIFF files were converted to 8-bit images and the distance of each pixel was defined as 1 pixel is equivalent to 0.107991 microns. This scale was defined as a global setting as individual images were processed into a binary image. Binary images were analyzed as particles with measurements recorded as perimeter and surface area. Recorded measurements were analyzed with Prism 5 for Windows Version 5.04 software (November 6, 2010).

Results

Localization of VAMP isoforms during platelet spreading

Distinct VAMP isoforms associated with specific vesicle subpopulations mediate the recruitment of membrane to growing actin-based structures during neurite outgrowth and phagocytotic cup

Downloaded from http://ashpublications.net/blood/article-pdf/120/1/199/1356030/zh802712000199.pdf by guest on 20 May 2024

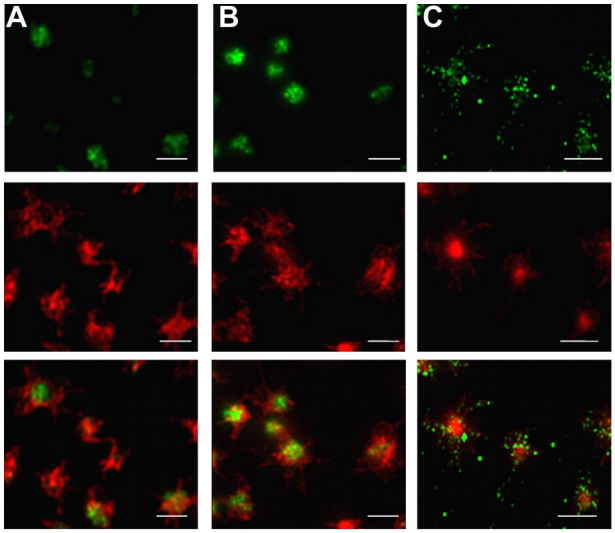

Figure 1. Localization of VAMP isoforms in spread platelets. Localization of VAMP isoforms was determined in spread platelets using double staining immunofluorescence microscopy. Spread platelets were labeled with antibodies to (A) VAMP-3, (B) VAMP-8, and (C) VAMP-7 followed by staining with secondary antibodies labeled with Alexa 488 (row 1). Platelets were costained with Alexa 546–phalloidin to visualize actin structures (row 2). Merged images were evaluated to determine the localization of VAMP isoforms relative to actin structures in spreading platelets (row 3). VAMP-3 and VAMP-8 localize to the center of the spread platelet, whereas VAMP-7 localizes to peripheral lamellipodia and pseudopodia. Scale bars, 5 μm.

formation.[22-24] The previous observation that a subset of platelet granules move to the periphery of the platelet during spreading whereas the remaining granules are sequestered in the granulomere[35,36] raised the question of whether these 2 populations express different VAMP isoforms. We evaluated the subcellular localization of VAMP-3 and VAMP-8 because these isoforms function in granule exocytosis.[2,31-33] We also evaluated the localization of VAMP-7, which contains an N-terminal longin domain with structural homology to profilin. Evaluation of resting platelets did not reveal any obvious differences in the distribution of these VAMP isoforms (supplemental Figure 2). To evaluate the localization of granules after spreading, platelets were plated on poly-L-lysine to minimize activation and counterstained with Alexa 568–conjugated phalloidin to facilitate visualization and identify actin structures. These studies demonstrated that VAMP-3 and VAMP-8 appeared in the center of the spread platelet consistent with localization to the central granulomere (Figure 1A-B). In contrast, VAMP-7 localized to the periphery of the spread platelet. In particular, VAMP-7 was observed at the edge of lamellipodia and tips of pseudopodia (Figure 1C). Pseudopodia and lamellipodia were nearly devoid of VAMP-3 and VAMP-8. These studies demonstrate differential localization of granule populations in spread platelets, with granules expressing VAMP-7 localized to the periphery of the spread platelet and granules expressing VAMP-3 and VAMP-8 localized to the central granulomere.

Further studies were performed to quantify the localization of VAMP isoforms in spread platelets and assess the localization of platelet cargos. The α-granule cargo, VWF, and the dense granule cargo, serotonin, were analyzed along with VAMP-8 and VAMP-7. For these analyses, the percentage of each label associated with the central granulomere versus the peripheral lamellipodia and pseudopodia was determined. Identification of the granulomere was performed using thresholding of F-actin staining and confirmed by brightfield images (supplemental Figure 2). A mask was drawn around the central granulomere and the percentage of fluorescence within and outside the mask was quantified using ImageJ. In these studies, 92 ± 6% of VAMP-8 (Figure 2A,G), 89 ± 4% of serotonin (Figure 2B,G), and 84 ± 6% of VWF (Figure 2C,G) remained in the central granulomere during spreading. In contrast, 78 ± 5% of VAMP-7 was observed in the periphery (Figure 2D,G). These experiments demonstrate that during spreading structures expressing VAMP-7 segregate from granules expressing VAMP-8, which localize to the granulomere.

Additional studies were performed to identify α-granule cargos that localize to the periphery with spreading. PDGF, PF4, and thrombospondin all localized to the central granulomere on spreading (supplemental Figure 3). In contrast, TIMP2 was found primarily in the periphery of spread platelets (Figure 2E,G). VEGF localized both to the periphery and granulomere (Figure 2F-G). TIMP2 and VEGF both colocalized with VAMP-7 in the periphery of spread platelets (Figure 3). In particular, TIMP2 localized to peripheral granules expressing VAMP-7 (Manders coefficient $[M_2] = 0.93 \pm 0.1$; Figure 3A). VEGF also localized with peripheral granules expressing VAMP-7 ($M_2 = 0.68 \pm 0.09$; Figure 3B). The supposition that granules expressing VAMP-7 are α-granules was supported by studies demonstrating the colocalization of VAMP-7 with P-selectin ($R_r = 0.63 \pm 0.9$; Figure 3C). These

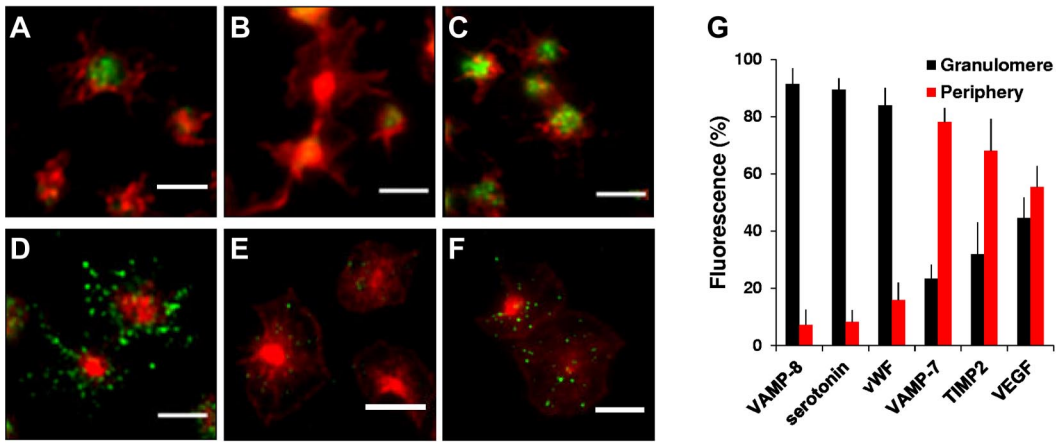

Figure 2. Quantitative analysis of VAMP isoforms and cargo in spread platelets. Double immunofluorescence microscopy of actin and (A) VAMP-8, (B) serotonin, (C) VWF, (D) VAMP-7, (E) TIMP2, or (F) VEGF. Scale bars, 5 μm. (G) Images were evaluated as described in supplemental Figure 3 to demarcate the granulomere of the spread platelets and subsequently analyzed to quantify the amount of VAMP-8, serotonin, VWF, VAMP-7, TIMP2, and VEGF associated with the granulomere (black) versus the periphery (red). Error bars represent the standard deviation (SD) of measurements from 250 to 350 platelets per condition.

Downloaded from http://ashpublications.net/blood/article-pdf/120/1/199/1356030/zh802712000199.pdf by guest on 20 May 2024

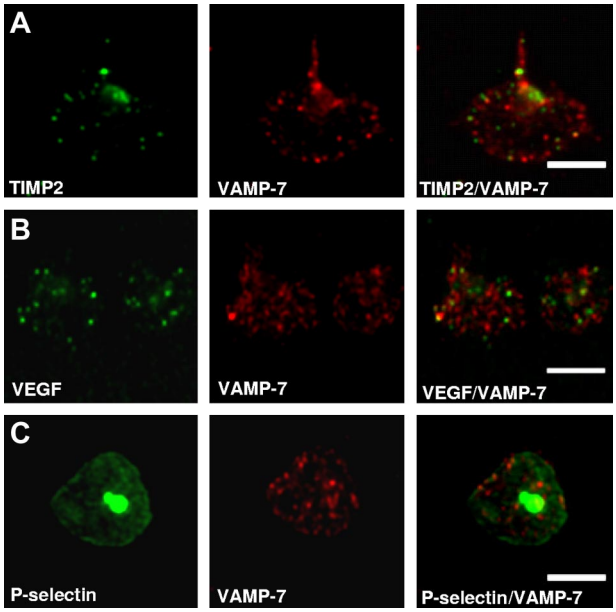

Figure 3. Colocalization studies demonstrate association of TIMP2, VEGF, and P-selectin with VAMP-7–expressing α-granules. Double fluorescence confocal microscopy of granules in spread platelets stained using antibodies to (A) anti-TIMP2, (B) anti-VEGF, or (C) P-selectin and counterstaining with anti–VAMP-7 antibody demonstrates peripheral colocalization of VAMP-7 with these α-granule markers. Scale bars, 5 μm.

results indicate that a VAMP-7–expressing α-granule subpopulation translocates to the periphery during platelet spreading.

Movement of granules during platelet spreading

Active translocation of vesicles to growing structures is observed in neurite outgrowth and development of the phagocytic cup in macrophages.[16-20] We used time-lapse microscopy to assess whether platelet granules move during spreading. Platelets were incubated with quantum dot 565 nanocrystals to load α-granules and enable visualization by fluorescent microscopy. After spreading on poly-L-lysine, the majority of granules remained in the central granulomere (Figure 4A). However, also observed was a population of granules in the periphery of spreading platelets. Time-lapse microscopy demonstrated that these peripheral granules moved in a somewhat erratic manner, but generally appeared to translocate from the central granulomere to the platelet periphery (Figure 4A-B). The rapid loss of granule signal between 60 to 90 seconds probably represents the exocytosis of the granule with loss of its contents. Alternatively, it could represent the movement of the granule in the z-axis, exiting the focal plane. Overall, these results demonstrate the active translocation of granules in spreading platelets and indicate that these granules move toward the periphery of the expanding platelet.

We used immunofluorescence confocal microscopy to characterize the population of granules that moved to the periphery over time. Platelets were loaded with quantum dot 565 nanocrystals and the colocalization of VAMP-7 with nanocrystals in the platelet periphery was evaluated (Figure 4C). These studies demonstrated substantial colocalization of VAMP-7 with quantum dot 565 nanocrystals in the periphery ($R_r = 0.89 \pm 0.07$). In particular, $92 \pm 5.6\%$ of quantum dot fluorescence colocalized with VAMP-7 fluorescence ($n = 61$ platelets). To determine whether granules that moved to the periphery were α-granules, quantum dot 565 nanocrystal-loaded platelets were costained with antibodies directed at P-selectin (Figure 4D). This evaluation demonstrated substantial colocalization of P-selectin and quantum dot nanocrystals in peripheral granules ($R_r = 0.92 \pm 0.04$). In particular, $94 \pm 2\%$ of quantum dot fluorescence colocalized with P-selectin ($n = 37$ platelets). These results indicate that α-granules expressing VAMP-7 move to the platelet periphery during spreading.

Role of granule secretion in platelet spreading

The supposition that granule exocytosis contributes to platelet spreading has not previously been assessed directly, and whether

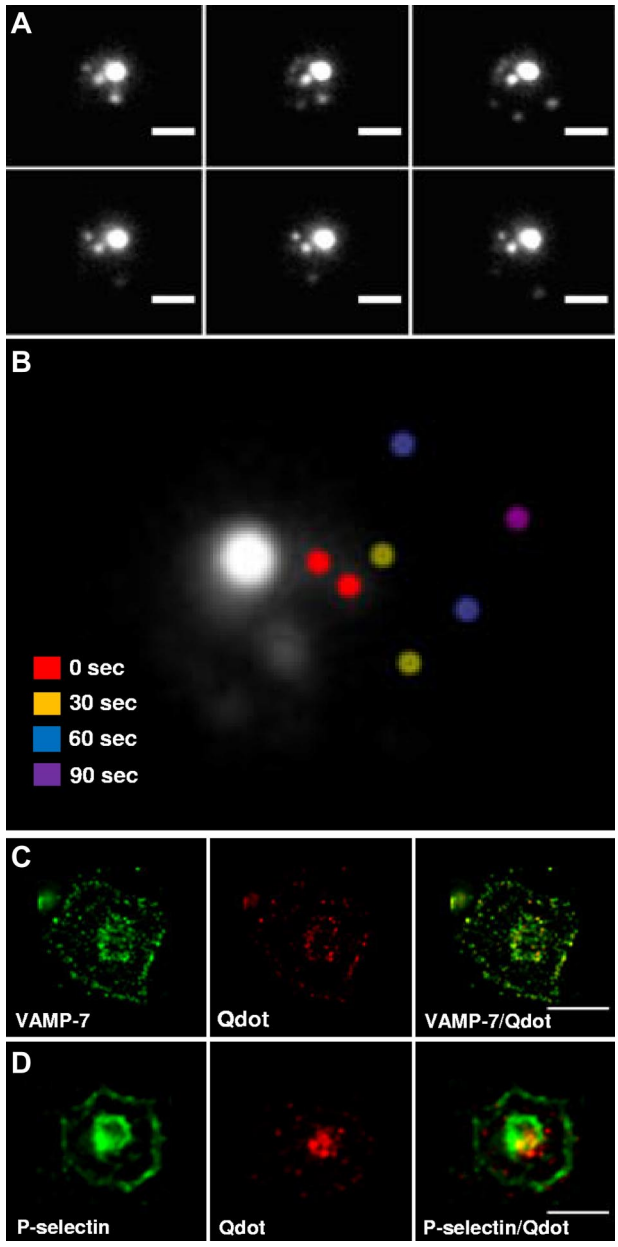

Figure 4. Time-lapse microscopy of platelet α-granule movement during spreading. (A) Platelets were loaded with quantum dot 565 nanocrystals overnight and visualized during spreading on poly-L-lysine. Images were obtained every 30 seconds during spreading. Scale bar, 2.5 μm. (B) Images were taken immediately after adhesion (0 seconds) and at the indicated times thereafter. An overlay of a representative series of images demonstrates that the majority of the fluorescence remains localized to the central granulomere. However, movement of peripheral granules could be visualized. Peripheral granules imaged at different time points were pseudocolored to indicate position: 0 seconds (red), 30 seconds (yellow), 60 seconds (blue), and 90 seconds (purple). (C) Double fluorescence confocal microscopy of granules in spread platelets using anti–VAMP-7 antibody and endocytosed quantum dot 565 nanocrystals demonstrates peripheral colocalization of VAMP-7 with nanocrystals. (D) Double immunofluorescence staining of spread platelets demonstrates colocalization of P-selectin with quantum dot 565 nanocrystals in the platelet periphery. Scale bars, 5 μm.

Downloaded from http://ashpublications.net/blood/article-pdf/120/1/199/1356030/zh802712000199.pdf by guest on 20 May 2024

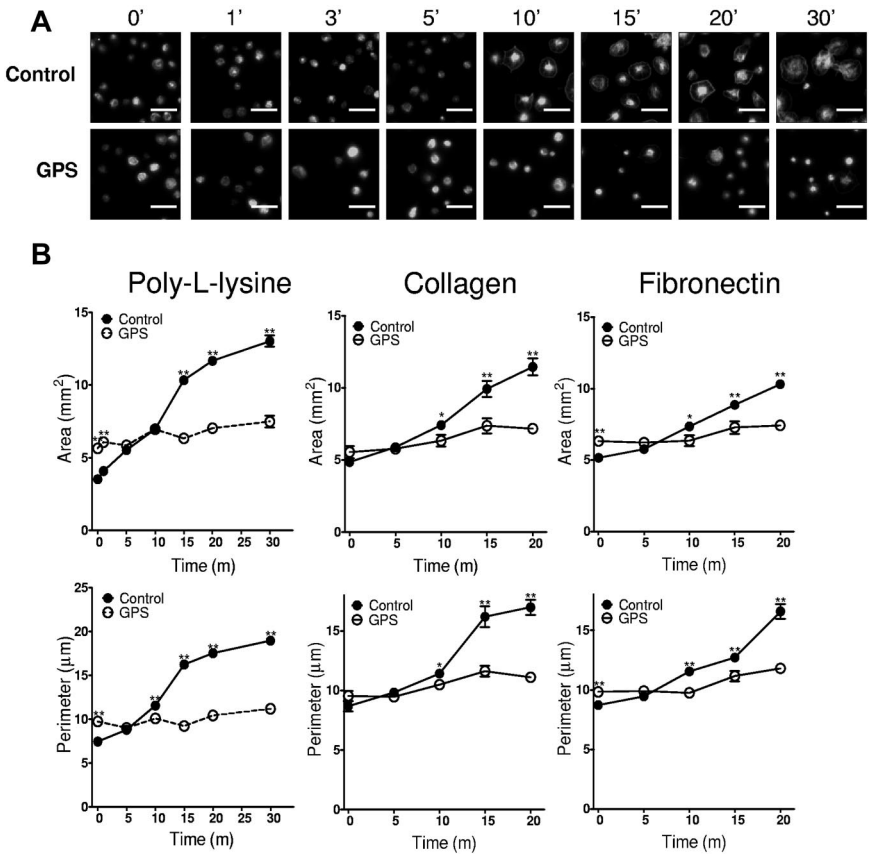

Figure 5. GPS platelets demonstrate a spreading defect. (A) Fluorescence microscopy of control and GPS platelets spread for the indicated amounts of time on poly-L-lysine and stained with Alexa 546–phalloidin. (B) Quantification of surface area and perimeter of spread platelets from control (solid circles, solid lines) and GPS (open circles, dashed lines) subjects spread on either poly-L-lysine, collagen, or fibronectin as indicated. Error bars represent the standard error of the mean (SEM) of measurements from 150 to 250 platelets per time point.

this process is required for normal platelet spreading is unknown. To determine whether platelet granules contribute to spreading, we evaluated platelet spreading in a patient with HPS and in a patient with GPS. HPS platelets are deficient in platelet dense granules, but have normal size α-granules. There was no difference in spreading between HPS platelets and platelets from healthy controls (supplemental Figure 4). Patients with GPS have macrothrombocytopenia and platelets that lack normal α-granules, but have normal dense granules. GPS platelets demonstrated increased surface area and perimeter on initial seeding on poly-L-lysine, collagen, or fibronectin because of their large size (Figure 5B; time 0). However, GPS platelets failed to spread significantly over time, whereas platelets from a healthy control demonstrated a ~ 3- to 4-fold increase in surface area and perimeter (Figure 5B). This result raises the possibility that α-granules function in spreading.

The ability of platelets from *Unc13d*^{Jinx} mice to spread was next assessed to determine whether granule exocytosis is required for normal spreading. *Unc13d*^{Jinx} platelets have normal VAMP isoform expression (supplemental Figure 5), but demonstrate markedly impaired granule membrane fusion because of a deficiency in Munc13-4,[38] a Rab27a effector protein that is mutated in familial hemophagocytotic lymphohistiocytosis 3.[39-41] They demonstrate a defect in both dense granule and α-granule exocytosis, but are otherwise normal. After plating on poly-L-lysine, collagen, or fibronectin-coated coverslips, wild-type platelets spread during a 15 minute time period, with initial pseudopodia extension followed by lamellipodia formation (Figure 6A). In contrast, *Unc13d*^{Jinx} platelets demonstrated delayed and reduced spreading during the same time period. By 10 minutes, significant lamellipodia formation had occurred in wild-type platelets, whereas the large majority of *Unc13d*^{Jinx} platelets remained rounded in shape. Quantification of these results using ImageJ 1.44p Java 1.6.0_20 (32 bit) software demonstrate delayed and decreased spreading of *Unc13d*^{Jinx} platelets compared with wild-type platelets (Figure 6B). These studies confirm a role for granule exocytosis in platelet spreading.

Discussion

Several recent studies indicate that platelets contain different subsets of α-granules. The majority of evidence suggesting the existence of multiple α-granule subtypes is derived from immunofluorescence of α-granule cargos demonstrating distinct localization.[6-8] The interpretation of these results has been questioned, however, in light of studies using high resolution immunofluorescence microscopy demonstrating that cargos are stochastically distributed among α-granules and that segregation within α-granules could be mistaken for segregation among α-granules.[11,12] One approach to address this concern is to physically separate α-granule subtypes. However, experimental strategies for separating α-granules based on cargo have not been described. Our studies show that the platelet itself physically sorts and separates α-granule subtypes during spreading.

Rather than identify α-granule subtypes based on cargo proteins, we initially addressed the question of α-granule heterogeneity by evaluating the localization of VAMPs, which are expressed on the cytosolic face of α-granules. An important function of VAMPs is to sort different granule types during granulogenesis, making them useful markers in identifying platelet α-granule subtypes. These results demonstrate that a subset of α-granules expressing VAMP-7 move to the periphery of the spreading platelet. In contrast, granules that express VAMP-3 and VAMP-8 localize to the central granulomere. Of note, the 2 VAMP isoforms that have been shown to mediate granule secretion, VAMP-3 and

Downloaded from http://ashpublications.net/blood/article-pdf/120/1/199/1356030/zh802712000199.pdf by guest on 20 May 2024

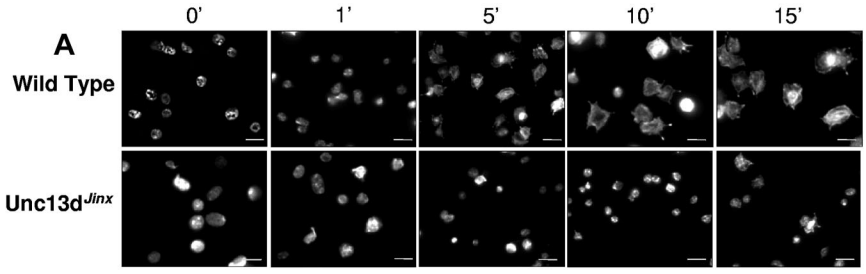

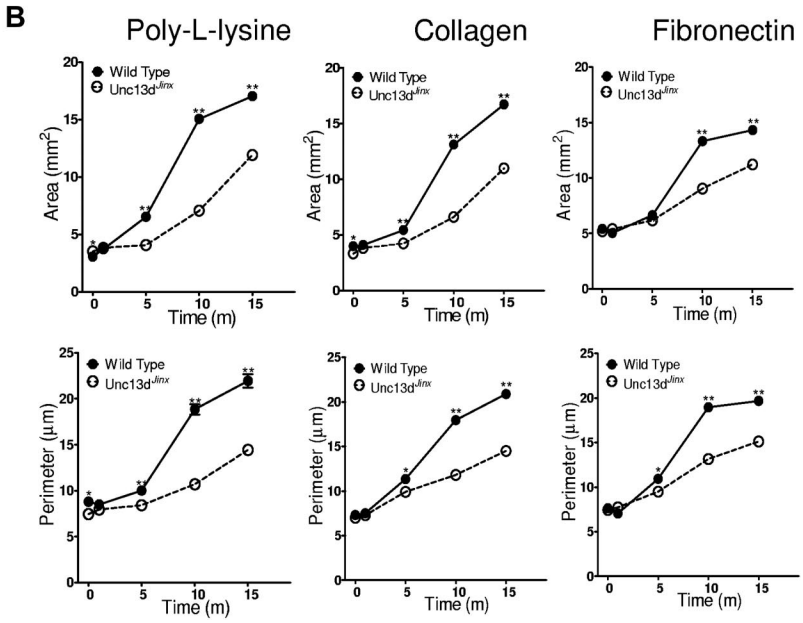

Figure 6. Platelets from *Unc13d*^{Jinx} mice demonstrate a spreading defect. (A) Fluorescence microscopy of platelets from wild-type and *Unc13d*^{Jinx} mice spread for the indicated amounts of time on poly-L-lysine and stained with Alexa 546–phalloidin. Scale bars, 5 μm. (B) Quantification of surface area and perimeter in platelets from wild-type (solid circles, solid lines) and Unc13d^{Jinx} (open circles, dashed lines) mice spread on either poly-L-lysine, collagen, or fibronectin as indicated. Error bars represent the SEM of measurements from 150 to 250 platelets per time point.

VAMP-8, are sequestered in the granulomere along with the granule cargos, VWF and serotonin. VAMP-7 translocates to the periphery of the platelet along with cargos, TIMP2 and VEGF. The physical separation of TIMP2 from VWF that we observed during spreading was consistent with the segregation of TIMP2 and VWF previously observed by Villeneuve et al.[42] The TIMP2-containing vesicular or granular structures identified in these studies were present in GPS platelets as well as platelets from normal individuals. Granules expressing VAMP-7 appear to deliver membrane to cover growing actin structures in the platelet periphery. However, the precise nature and function of the granular structures that express VAMP-7 and contain TIMP2 remains to be defined.

During spreading, the platelet undergoes a 2- to 4-fold increase in plasma membrane surface area as it transforms from a discoid cell to a flattened, irregular form with pseudopodia and lamellipodia.[43] The role of platelet granule exocytosis in the extensive membrane remodeling that occurs during spreading is largely unstudied. Our results show that platelet α-granules, but not dense granules, contribute to spreading. GPS platelets have defective α-granules and demonstrate markedly impaired spreading (Figure 5). In contrast, platelets from a patient with HPS whose platelets lack dense granules demonstrated normal spreading (supplemental Figure 4). The premise that granule exocytosis contributes to the growing plasma membrane at the periphery of the spreading platelet is further supported by the observation that membrane spreading is delayed and reduced in *Unc13d*^{Jinx} platelets (Figure 6), which have impaired granule secretion. *Unc13d*^{Jinx} mouse platelets lack the SNARE-associated protein Munc13-4. Munc13-4 is an essential component of the distal secretory machinery. Studies by Ren et al demonstrated that these platelets exhibit normal granule morphology and proximal signaling, but have a marked defect in the exocytosis of all 3 granule types.[38] Other than a deficiency in Munc13-4, these platelets possess a normal secretory machinery and granule content. Therefore, it is unlikely that the defect in spreading in *Unc13d*^{Jinx} platelets is secondary to granule deficiency or impaired proximal signaling mechanisms.

Although the mechanisms that link granule exocytosis with platelet spreading remain uncertain, our results implicate VAMP-7 in this process. VAMP-7 is widely expressed in cells and is present in platelets at 3766 + 696 molecules/platelet.[2] VAMP-7 is unique among platelet VAMPs in that it is the only VAMP that possesses an N-terminal, profilin-like longin domain.[44,45] Profilin binds G-actin and Arp2/3, promoting actin polymerization. In nucleated cells, VAMP-7 functions in membrane remodeling in the context of dynamic actin polymerization. VAMP-7 has been implicated in delivering granules to provide auxiliary membrane to the leading edge of the plasma membrane during cell migration.[22-24] VAMP-7 mediates membrane fusion required for tubulovesicular structures at the leading edge of elongating dendrites and axons that support neurite outgrowth.[16-18] VAMP-7 also functions in the delivery of granules to the phagocytotic cup in macrophages.[19,20] A signaling pathway has been described in which integrin-dependent activation leads to the coordinated activity of Arp2/3 complex-mediated actin polymerization and VAMP-7–mediated exocytosis in neurite outgrowth.[18,46] In platelets, granules expressing VAMP-7 may preferentially translocate to the periphery via an

Downloaded from http://ashpublications.net/blood/article-pdf/120/1/199/1356030/zh802712000199.pdf by guest on 20 May 2024

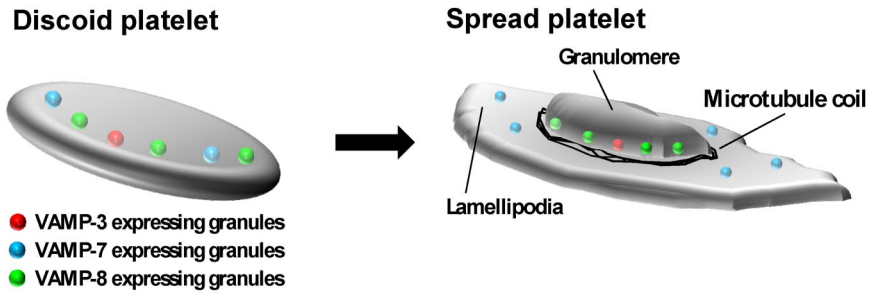

Figure 7. Model of α-granule movement during platelet spreading. In the resting platelet, α-granules expressing VAMP-3, VAMP-7, and VAMP-8 are dispersed throughout the platelet. During platelet spreading, granules expressing VAMP-3 and VAMP-8 localize to the central granulomere surrounded by a microtubule ring. Granules expressing VAMP-7 move toward the platelet periphery. Exocytosis of granules contributes to expansion of the plasma membrane during spreading.

actin-dependent process in which VAMP-7 participates in actin nucleation that propels the granule. Alternatively, VAMP-7 may simply be a marker for granules that translocate by an unrelated mechanism. Further studies will be required to distinguish between these possibilities.

Our results suggest a model for the role of granule exocytosis in platelet spreading. We propose that in resting platelets, α-granules expressing different VAMPs are dispersed throughout the platelet. During spreading, a subpopulation of granules that express VAMP-7 are preferentially recruited to the platelet periphery. We speculate that these granules fuse at the periphery and add membrane to developing pseudopodia and lamellipodia (Figure 7). In contrast, granules expressing VAMP-3 and VAMP-8, which colocalize with granule cargos, are sequestered in the central granulomere (Figure 7). Thus, distinct granule populations distinguished by expression of different VAMP isoforms serve different functions during platelet spreading.

In summary, we have shown that granule exocytosis is required for platelet spreading and identified a new α-granule subtype that expresses VAMP-7 and moves to the periphery during spreading. This observation is consistent with the proposal that α-granules are heterogeneous and demonstrates that different VAMP isoforms localize to functionally discrete α-granule subtypes.

Acknowledgments

The authors thank Joseph E. Italiano, PhD and Jonathan N. Thon, PhD for providing guidance with microscopy, and Nathalie A. Fadel for artwork.

This work was supported by National Institutes of Health grant HL087203 (R.F.). C.G.P. was supported by T32 HL07917. R.F. is a recipient of an Established Investigator Award from the American Heart Association.

Authorship

Contribution: C.G.P. designed and performed research, analyzed data, and contributed to writing the paper; A.D.M. assisted in designing and performing experiments involving the GPS patient and contributed to writing the paper; and R.F. conceived of study, designed studies, analyzed data, and wrote the paper.

Conflict-of-interest disclosure: The authors declare no competing financial interests.

Correspondence: Robert Flaumenhaft, Center for Life Science, Rm 939, Beth Israel Deaconess Medical Center, 3 Blackfan Cir, Boston, MA, 02215; e-mail: rflaumen@bidmc.harvard.edu.

References

1. Swank RT, Novak EK, McGarry MP, Rusiniak ME, Feng L. Mouse models of Hermansky Pudlak syndrome: a review. *Pigment Cell Res.* 1998; 11(2):60-80.
2. Graham GJ, Ren Q, Dilks JR, Blair P, Whiteheart SW, Flaumenhaft R. Endobrevin/VAMP-8-dependent dense granule release mediates thrombus formation in vivo. *Blood.* 2009;114(5):1083-1090.
3. Ho-Tin-Noé B, Goerge T, Cifuni SM, Duerschmied D, Wagner DD. Platelet granule secretion continuously prevents intratumor hemorrhage. *Cancer Res.* 2008; 68(16):6851-6858.
4. Blair P, Flaumenhaft R. Platelet alpha-granules: basic biology and clinical correlates. *Blood Rev.* 2009;23(4):177-189.
5. van Nispen tot Pannerden H, de Haas F, Geerts W, Posthuma G, van Dijk S, Heijnen HF. The platelet interior revisited: electron tomography reveals tubular alpha-granule subtypes. *Blood.* 2010;116(7):1147-1156.
6. Sehgal S, Storrie B. Evidence that differential packaging of the major platelet granule proteins von Willebrand factor and fibrinogen can support their differential release. *J Thromb Haemost.* 2007;5(10):2009-2016.
7. Italiano JE Jr, Richardson JL, Patel-Hett S, et al. Angiogenesis is regulated by a novel mechanism: pro- and antiangiogenic proteins are organized into separate platelet {alpha} granules and differentially released. *Blood.* 2008;111(3):1227-1233.
8. Chatterjee M, Huang Z, Zhang W, et al. Distinct platelet packaging, release, and surface expression of proangiogenic and antiangiogenic factors on different platelet stimuli. *Blood.* 2011;117(14): 3907-3911.
9. Ma L, Perini R, McKnight W, et al. Proteinase-activated receptors 1 and 4 counter-regulate endostatin and VEGF release from human platelets. *Proc Natl Acad Sci U S A.* 2005;102(1):216-220.
10. Battinelli EM, Markens BA, Italiano JE Jr. Release of angiogenesis regulatory proteins from platelet alpha granules: modulation of physiologic and pathologic angiogenesis. *Blood.* 2011;118(5): 1359-1369.
11. Kamykowski J, Carlton P, Sehgal S, Storrie B. Quantitative immunofluorescence mapping reveals little functional coclustering of proteins within platelet alpha-granules. *Blood.* 2011; 118(5):1370-1373.
12. Whiteheart SW. Platelet granules: surprise packages. *Blood.* 2011;118(5):1190-1191.
13. Bretscher MS. Moving membrane up to the front of migrating cells. *Cell.* 1996;85(4):465-467.
14. Steinhardt RA, Bi G, Alderton JM. Cell membrane resealing by a vesicular mechanism similar to neurotransmitter release. *Science.* 1994; 263(5145):390-393.
15. Bi GQ, Alderton JM, Steinhardt RA. Calcium-regulated exocytosis is required for cell membrane resealing. *J Cell Biol.* 1995;131(6 Pt 2): 1747-1758.
16. Martinez-Arca S, Alberts P, Zahraoui A, Louvard D, Galli T. Role of tetanus neurotoxin insensitive vesicle-associated membrane protein (TI-VAMP) in vesicular transport mediating neurite outgrowth. *J Cell Biol.* 2000;149(4):889-900.
17. Martinez-Arca S, Coco S, Mainguy G, et al. A common exocytotic mechanism mediates axonal and dendritic outgrowth. *J Neurosci.* 2001;21(11): 3830-3838.
18. Alberts P, Rudge R, Irinopoulou T, Danglot L, Gauthier-Rouviere C, Galli T. Cdc42 and actin control polarized expression of TI-VAMP vesicles to neuronal growth cones and their fusion with the plasma membrane. *Mol Biol Cell.* 2006;17(3): 1194-1203.
19. Braun V, Fraisier V, Raposo G, et al. TI-VAMP/VAMP7 is required for optimal phagocytosis of opsonised particles in macrophages. *EMBO J.* 2004;23(21):4166-4176.
20. Braun V, Niedergang F. Linking exocytosis and endocytosis during phagocytosis. *Biol Cell.* 2006; 98(3):195-201.
21. Gupton SL, Gertler FB. Integrin signaling switches the cytoskeletal and exocytic machinery that drives neuritogenesis. *Dev Cell.* 2010;18(5): 725-736.
22. Luftman K, Hasan N, Day P, Hardee D, Hu C. Silencing of VAMP3 inhibits cell migration and integrin-mediated adhesion. *Biochem Biophys Res Commun.* 2009;380(1):65-70.
23. Proux-Gillardeaux V, Gavard J, Irinopoulou T,

Downloaded from http://ashpublications.net/blood/article-pdf/120/1/199/1356030/zh802712000199.pdf by guest on 20 May 2024

Mege RM, Galli T. Tetanus neurotoxin-mediated cleavage of cellubrevin impairs epithelial cell migration and integrin-dependent cell adhesion. *Proc Natl Acad Sci U S A.* 2005;102(18):6362-6367.

24. Proux-Gillardeaux V, Raposo G, Irinopoulou T, Galli T. Expression of the Longin domain of TI-VAMP impairs lysosomal secretion and epithelial cell migration. *Biol Cell.* 2007;99(5):261-271.
25. Tiwari N, Wang CC, Brochetta C, et al. VAMP-8 segregates mast cell-preformed mediator exocytosis from cytokine trafficking pathways. *Blood.* 2008;111(7):3665-3674.
26. Puri N, Roche PA. Mast cells possess distinct secretory granule subsets whose exocytosis is regulated by different SNARE isoforms. *Proc Natl Acad Sci U S A.* 2008;105(7):2580-2585.
27. Pocard T, Le Bivic A, Galli T, Zurzolo C. Distinct v-SNAREs regulate direct and indirect apical delivery in polarized epithelial cells. *J Cell Sci.* 2007; 120(Pt 18):3309-3320.
28. Weng N, Thomas DD, Groblewski GE. Pancreatic acinar cells express vesicle-associated membrane protein 2- and 8-specific populations of zymogen granules with distinct and overlapping roles in secretion. *J Biol Chem.* 2007;282(13): 9635-9645.
29. Steegmaier M, Lee KC, Prekeris R, Scheller RH. SNARE protein trafficking in polarized MDCK cells. *Traffic.* 2000;1(7):553-560.
30. Jahn R, Scheller RH. SNAREs–engines for membrane fusion. *Nat Rev Mol Cell Biol.* 2006;7(9): 631-643.
31. Feng D, Crane K, Rozenvayn N, Dvorak AM, Flaumenhaft R. Subcellular distribution of 3 functional platelet SNARE proteins: human cellubrevin, SNAP-23, and syntaxin 2. *Blood.* 2002; 99(11):4006-4014.
32. Polgár J, Chung SH, Reed GL. Vesicle-associated membrane protein 3 (VAMP-3) and VAMP-8 are present in human platelets and are required for granule secretion. *Blood.* 2002;100(3):1081-1083.
33. Ren Q, Barber HK, Crawford GL, et al. Endobrevin/VAMP-8 is the primary v-SNARE for the platelet release reaction. *Mol Biol Cell.* 2007; 18(1):24-33.
34. Loftus JC, Choate J, Albrecht RM. Platelet activation and cytoskeletal reorganization: high voltage electron microscopic examination of intact and Triton-extracted whole mounts. *J Cell Biol.* 1984; 98(6):2019-2025.
35. Fritz M, Radmacher M, Gaub HE. Granula motion and membrane spreading during activation of human platelets imaged by atomic force microscopy. *Biophys J.* 1994;66(5):1328-1334.
36. Allen RD, Zacharski LR, Widirstky ST, Rosenstein R, Zaitlin LM, Burgess DR. Transformation and motility of human platelets: details of the shape change and release reaction observed by optical and electron microscopy. *J Cell Biol.* 1979;83(1):126-142.
37. Dowal L, Sim DS, Dilks JR, et al. Identification of an antithrombotic allosteric modulator that acts through helix 8 of PAR1. *Proc Natl Acad Sci U S A.* 2011;108(7):2951-2956.
38. Ren Q, Wimmer C, Chicka MC, et al. Munc13-4 is a limiting factor in the pathway required for platelet granule release and hemostasis. *Blood.* 2010; 116(6):869-877.
39. Neeft M, Wieffer M, de Jong AS, et al. Munc13-4 is an effector of rab27a and controls secretion of lysosomes in hematopoietic cells. *Mol Biol Cell.* 2005;16(2):731-741.
40. Elstak ED, Neeft M, Nehme NT, et al. The munc13-4-rab27 complex is specifically required for tethering secretory lysosomes at the plasma membrane. *Blood.* 2011;118(6):1570-1578.
41. Feldmann J, Callebaut I, Raposo G, et al. Munc13-4 is essential for cytolytic granules fusion and is mutated in a form of familial hemophagocytic lymphohistiocytosis (FHL3). *Cell.* 2003; 115(4):461-473.
42. Villeneuve J, Block A, Le Bousse-Kerdiles MC, et al. Tissue inhibitors of matrix metalloproteinases in platelets and megakaryocytes: a novel organization for these secreted proteins. *Exp Hematol.* 2009;37(7):849-856.
43. Frojmovic MM, Milton JG. Human platelet size, shape, and related functions in health and disease. *Physiol Rev.* 1982;62(1):185-261.
44. Pryor PR, Jackson L, Gray SR, et al. Molecular basis for the sorting of the SNARE VAMP7 into endocytic clathrin-coated vesicles by the ArfGAP Hrb. *Cell.* 2008;134(5):817-827.
45. Pryor PR, Mullock BM, Bright NA, et al. Combinatorial SNARE complexes with VAMP7 or VAMP8 define different late endocytic fusion events. *EMBO Rep.* 2004;5(6):590-595.
46. Rossi V, Banfield DK, Vacca M, et al. Longins and their longin domains: regulated SNAREs and multifunctional SNARE regulators. *Trends Biochem Sci.* 2004;29(12):682-688.

Downloaded from http://ashpublications.net/blood/article-pdf/120/1/199/1356030/zh802712000199.pdf by guest on 20 May 2024